VOL. 16, NO. 3, FEBRUARY 2021 ISSN 1819-6608
ARPN Journal of Engineering and Applied Sciences

www.arpnjournals.com

FINDING THE WATERFRONT RADIUS IN WATERFLOOD PROJECTS FROM WELL TEST INTERPRETATION

Freddy Humberto Escobar[1], Angela Maria Palomino[1] and Daniel Suescún-Díaz[2]
[1]Universidad Surcolombiana / CENIGAA, Avenida Pastrana - Cra, Neiva, Huila, Colombia
[2]Departamento de Ciencias Naturales, Avenida Pastrana, Universidad Surcolombiana, Neiva, Huila, Colombia
E-Mail: fescobar@usco.edu.co

ABSTRACT

Determination of the radius on the invasion front is important for appropriate management of waterflood projects. Currently, there is no analytical technique available for such purpose and the only way to be performed is by means of commercial well test software by reading the position of the investigation radius on the computer screen. Several models have been presented in the literature to account for pressure behavior on injection and falloff tests. In this work, one of the models is taken to study pressure and pressure derivative behavior so expressions to find the invasion front position are developed by detecting characteristic points and features on the pressure derivative versus time log-log plot, following the philosophy of the *TDS* Technique. Equations for the straight-line conventional analysis are also developed. The equations of both techniques are successfully verified on synthetic examples.

Keywords: injection front, non-unit mobility ratio, *TDS* Technique, conventional analysis, radial flow regime.

1. INTRODUCTION

Normally, waterflooding projects are initiated once the reservoir has produced enough time to reach depletion. Waterflood mechanism purpose is twofold: a) to provide the reservoir with energy, b) to displace the oil left behind after a primary recovery process. Therefore, it is truly important to estimate the invaded waterfront position since once this reaches the production well, water cut increases rapidly; therefore, adequate management requires quick and appropriate estimation of the injection front position.

Pressure behavior in water flood projects have been extensively studied in the hydrocarbon literature. Several mathematical models have been provided to account for pressure behavior in secondary recovery tests. Some of the consider unitary mobility ratio and other consider non-unit mobility ratio. Others consider isothermal processes and others do not.

Woodward and Thambynayagam (1983) provided a line-source solution model for a non-isothermal system, meaning non-unitary mobility ratio, to account for pressure behavior in water flood projects. Their model has the disadvantage of low accuracy at very early time because of the line-source solution. However, it works well at late time which is important to determine the position of the waterfront. They also provided straight-line conventional analysis to determine fluid effective permeabilities, mobility ratio and skin factors. They applied their developed equations to several oil-field examples.

A similar work as the previous was presented by Woodward (1983) for bounded reservoirs drained by a partially-penetrating well. He provided straight-line conventional analysis and applied it to oil-field examples.
Bratvold and Horne (1990) presented a pressure solution for non-isothermal case when a hot reservoir is subjected to cold water injection. It considers the relative permeability characteristics of the porous medium related to the changes in fluid mobility impacted by the temperature. A studied by Escobar, Martinezand Bonilla, (2011) may provide an interpretation technique which should be helpful for this case.

Levitan (2002) introduced a well pressure model considering two-rate variable problem and did not provide interpretation technique, so his examples were performed by history matching. A studied of variable injection rate was conducted by Hachlaf, Tiab and Escobar (2002). They did provide an interpretation procedure by means of the *TDS* technique, Tiab (1995) and demonstrated its accuracy on actual field data examples.

More pressure behavior solutions have been presented by Habte and Onur (2014), Peres *et al.* (2004), Peres, Boughrara, and Reynolds (2006), Banerjee, Thompson and Reynolds (1998) and Bittencourt Neto *et al*. (2020) among others.

Jokhio *et al.* (2001) used the model originally introduced by Woodward and Thambynayagam (1983) to develop an interpretation methodology based upon the *TDS* Technique. They found expressions to estimate the phase permeabilities, skin factor and mobility reading characteristic points found on the pressure and pressure derivative versus time log-log plot. However, they did not provide the estimation of the waterfront position. Therefore, this work is a complementary material of Jokhio *et al*.'s (2002) work to determine the radius from the well to the position of the invaded front by using both *TDS* Technique and conventional analysis. The expressions were successfully applied to synthetic well test examples.

2. MATHEMATICAL TREATMENT

The mathematical model adopted in this study was presented by Woodward and Thambynayagam (1983) which considered line-source solution as given below:

$$P_i - P_{wf} = \frac{70.6 q_w \mu_w B_w}{k_w h} \left[\begin{array}{l} E\left(-\frac{r_{wb}^2}{4r_{tw}^2}\right) - E\left(-\frac{r_w^2}{4r_{to}^2}\right) \\ -Me^{-\left(\frac{r_{wb}^2}{4r_{tw}^2} - \frac{r_{wb}^2}{4r_{to}^2}\right)} E\left(-\frac{r_{wb}^2}{4r_{tw}^2}\right) \end{array} \right] \quad (1)$$

The following variables are defined:

$$r_{tw}^2 = \frac{0.0002637 k_w t}{\phi \mu_w c_1} \quad (2)$$

$$r_{to}^2 = \frac{0.0002637 k_o t}{\phi \mu_o c_2} \quad (3)$$

$$r_{wb}^2 = -\frac{q B_w t}{13.428\ h(S_{wi} - S_w)} + r_F^2 \quad (4)$$

$$c_1 = c_w S_w + (1 - S_w) c_o + c_f \quad (5)$$

$$c_2 = c_o S_o + (1 - S_o) c_w + c_f \quad (6)$$

The dimensionless pressure, pressure derivative and time are given as:

$$P_D = \frac{k_w h (P_i - P)}{141.2 q_w \mu_w B_w} \quad (7)$$

$$t_D * P_D' = \frac{k_w h (t * \Delta P')}{141.2 q_w \mu_w B_w} \quad (8)$$

$$t_D = \frac{0.0002637 k_w t}{\phi \mu_w c_t r_w^2} \quad (9)$$

Also, the mobility ratio defined as the mobility of displacing phase over the mobility of the displaced phase is defined as:

$$M = \frac{k_w / \mu_w}{k_o / \mu_o} \quad (10)$$

2.1 *TDS* Technique Formulation

Dimensionless pressure, pressure derivative and second pressure derivative against dimensionless time obtained from Equation (1) is given in Figure-1 for different invaded front radii and a mobility ratio of 20. Figure-2 expresses the same behavior but for a mobility ratio of 0.05. In the first case a plateau is observed crossing the pressure derivative at a value of one. However, if the mobility ratio increases so does the constant pressure derivative in this region (see Figure-3). This region, labeled as region 1, corresponds to radial flow regime along the invaded zone. A transition occurs when the injection front has been reached and another flat portion of radial flow regime follows. This always crosses the dimensionless pressure derivative axis at a value of one half. This second region, labeled as region 2, corresponds to radial flow during the uninvaded zone, meaning the oil zone.

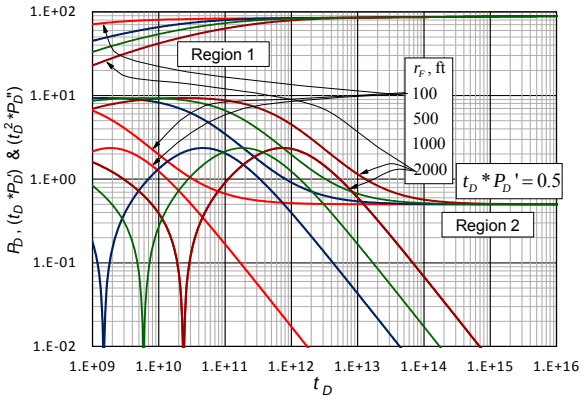

Figure-1. Dimensionless pressure, pressure derivative and second pressure derivative against dimensionless time for different radii and $M = 20$.

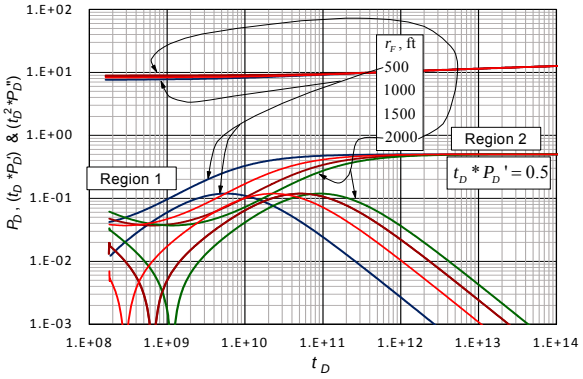

Figure-2. Dimensionless pressure, pressure derivative and second pressure derivative against dimensionless time for different radii and $M = 0.05$.

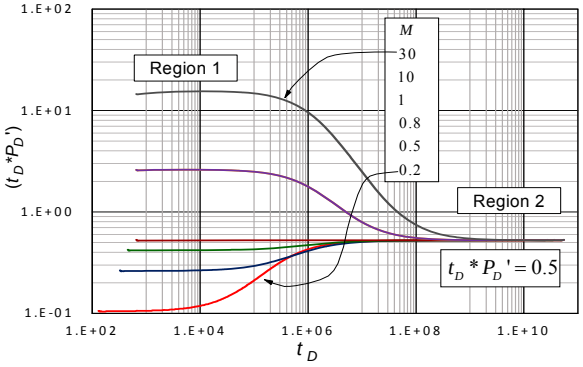

Figure-3. Dimensionless pressure derivative against dimensionless time for different mobility ratios and an invaded front radius, $r_F = 1000$ ft.

For the application of the *TDS* technique, Tiab (1995), there is a need of obtaining characteristic features or points on the pressure and pressure derivative log-log plot. For the cases provided in Figures 1, 2 and 3, the normalized or unified curves are provided in Figures 4 through 6.

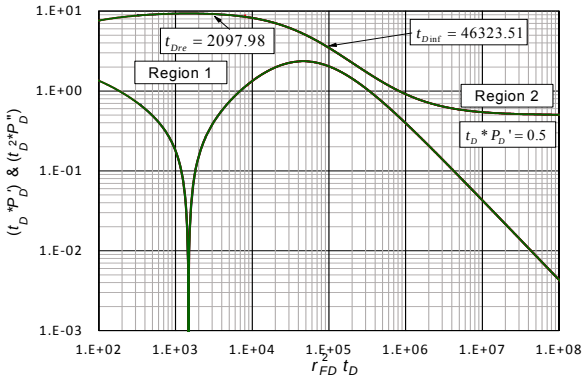

Figure-4. Normalized dimensionless pressure and pressure derivative against dimensionless time multiplied by the dimensionless radii of the invaded front for an adverse mobility ratio, $M = 20$.

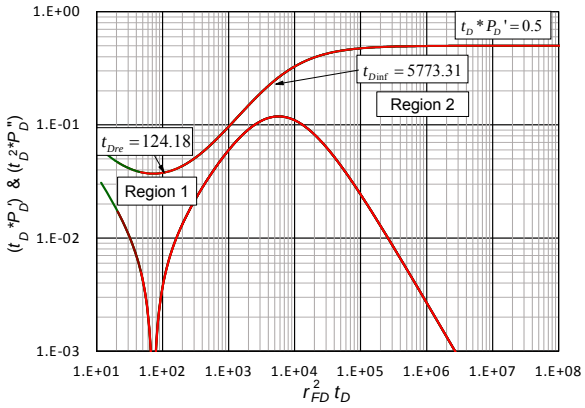

Figure-5. Normalized dimensionless pressure and pressure derivative against dimensionless time multiplied by the dimensionless radii of the invaded front for a favorable mobility ratio, $M = 0.05$.

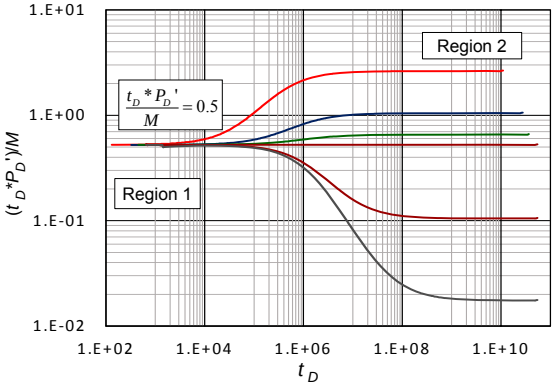

Figure-6. Normalized dimensionless pressure derivative divided by M against dimensionless time for different mobility ratios and an invaded front radius, $r_F = 1000$ ft.

According to Figure-6, during the invaded zone:

$$\left(\frac{t_D * P_D'}{M}\right)_{r1} = \frac{k_w h(t*\Delta P')}{141.2 q_w \mu_w B_w} = 0.5 \tag{11}$$

Solving for the effective water permeability,

$$k_w = \frac{70.6 q_w \mu_w B_w M}{h(t*\Delta P')} \tag{12}$$

It follows from Figure-1 through 5that during the uninvaded zone:

$$\left(t_D * P_D'\right)_{r2} = \frac{k_w h(t*\Delta P')}{141.2 q_w \mu_w B_w} = 0.5 \tag{13}$$

Then,

$$k_w = \frac{70.6 q_w \mu_w B_w}{h(t*\Delta P')_{r2}} \tag{14}$$

Solving from Equation (14) for the water mobility,

$$\frac{k_w}{\mu_w} = \frac{70.6 q_w B_w}{h(t*\Delta P')_{r2}} \tag{15}$$

Combining of Equations (10) and (15),

$$M\frac{k_o}{\mu_o} = \frac{70.6 q_w B_w}{h(t*\Delta P')_{r2}} \tag{16}$$

Once solving for the oil effective permeability, it yields:

$$k_o = \frac{70.6 q_w \mu_o B_w}{h(t*\Delta P')_{r2} M} \quad (16)$$

Equations (12), (14) and (16) were also reported by Jokhio *et al*. (2001) by taking the derivative to the solution of Equation (1) applied separately to regions 1 and 2.

From observation of Figures 4 and 5, the end of the radial flow regime of region 1 takes place once the invaded front radius is detected by the pressure transient wave, which always corresponds to a constant value:

$$r_{FD}^2 t_{Dre} = \text{constant} \quad (17)$$

Combination of Equations (17) and (9) allows finding an expression for the determination of the invaded front position, r_F, so:

$$r_F = \frac{1}{\xi}\sqrt{\frac{k_w t_{re}}{\phi \mu_w c_t}}, \quad \begin{cases} \xi = 2820.627 \text{ for } M > 1 \\ \xi = 686.232 \text{ for } M < 1 \end{cases} \quad (18)$$

Sometimes, determination of t_{re} results difficult, especially when noisy pressure derivative data are dealt with. In such cases, it is highly recommended using the inflection point formed between the two plateaus. This value can be easily read from the maximum point found on the second pressure derivative. It follows also from Figures 4 and 5, that:

$$r_{FD}^2 t_{D\inf} = \text{constant} \quad (19)$$

Also, a combination of Equations (19) and (9) leads to develop an equation for the determination of the invaded waterfront position, r_F,

$$r_F = \frac{1}{\xi}\sqrt{\frac{k_w t_{\inf}}{\phi \mu_w c_t}}, \quad \begin{cases} \xi = 13253.96 \text{ for } M > 1 \\ \xi = 4679.05 \text{ for } M < 1 \end{cases} \quad (20)$$

2.2 Straight-Line Conventional Analysis

Along with their model, Woodward and Thambynayagam (1983) also presented conventional analysis for interpretation of injection and falloff pressure tests for the determination of effective permeabilities, skin factors and mobility ratio. They did not provide a means for the estimation of the position of the invaded front.

A procedure like the one followed for the determination of the distance from a well to a sealing fault is used in this work. From the semi logarithmic plots given in Figures 7 and 8, we observe that the extrapolation of the radial semi logarithmic straight lines drawn on the first and second region, respectively, is about the same. In other words, extending the straight lines of the radial flow during regions 1 and 2 will provide an artificial point, t_x, which enables us to estimate the invaded radius. From these two plots, it is found that:

$$r_{FD}^2 t_{Dx} = \text{constant} \quad (21)$$

Combining Equations (19) and (9) allows developing an expression for the determination of the invaded front radius, r_F,

$$r_F = \frac{1}{\xi}\sqrt{\frac{k_w t_x}{\phi \mu_w c_t}}, \quad \begin{cases} \xi = 13507.6 \text{ for } M > 1 \\ \xi = 5333.05 \text{ for } M < 1 \end{cases} \quad (22)$$

Equation (22) is also applicable to pressure falloff tests once the intercept time value, t_x, is solved from the Horner time, $(t_p+\Delta t_x)/\Delta t_x$.

3. EXAMPLES

Table-1 contains reservoir, fluid and well data for simulated worked examples.

3.1 Simulated Example 1

Figures-9 and -10 provide the information needed for example 1. This test should be interpreted for estimating effective water permeability, effective oil permeability, and the invaded front position.

3.1.1 Solution by *TDS* technique

The following information was read from Figure-9:

$(t*\Delta P')_{r1}$= 11.33 psi $(t*\Delta P')_{r2}$ = 1.2 psi
t_{re} = 10715 hr t_{inf} = 229100 hr

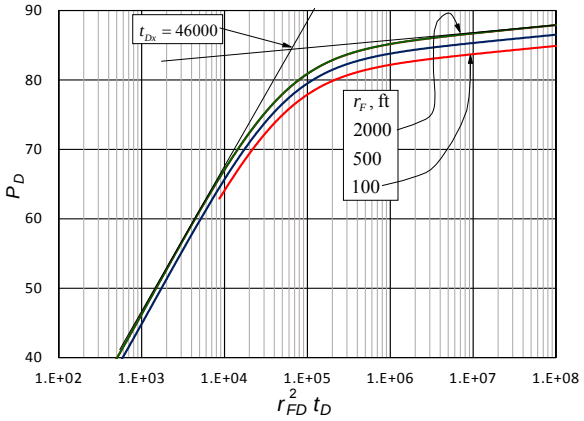

Figure-7. Dimensionless pressure against the logarithm of the dimensionless time multiplied by the dimensionless radius of the invaded front for an adverse mobility ratio, M = 20.

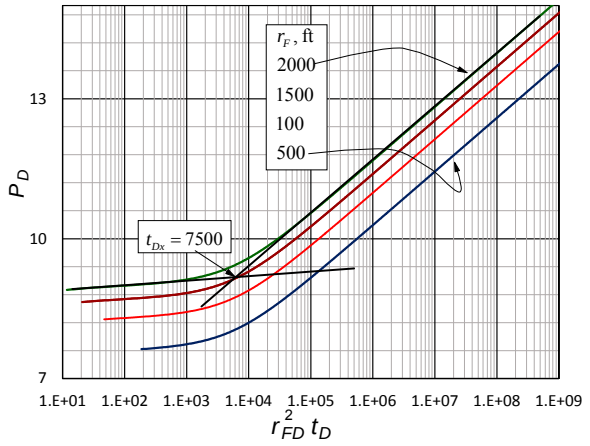

Figure-8. Dimensionless pressure against dimensionless time multiplied by the dimensionless radius of the invaded front for a favorable mobility ratio, $M = 0.05$.

The point read on pressure derivative during the first radial flow, water region, is used to determine effective water permeability from Equation (12);

$$k_w = \frac{70.6(10)(2500)(1)(1)}{(50)(11.33)} = 3115.62 \text{ md}$$

On the other hand, the point read on the pressure derivative curve during the second radial flow is used to find the effective oil permeability by using Equation (16);

$$k_o = \frac{70.6(2500)(3)(1)}{(50)(1.2)(10)} = 882.5 \text{ md}$$

Then, using the time at which the first radial flow ends, the invaded front position is found from Equation (18);

Table-1. Reservoir, fluid and well data for worked examples.

PARAMETER	Example 1	Example 2
q, STB/D	2500	6000
h, ft	50	30
ϕ, %	20	10
r_w, ft	0.3	
k, md	3000	
k_{ro}, md	0.3	
k_{rw}, md	1	
μ_o, cp	3	0.15
μ_w, cp	1	2
M	10	0.25
s_w,%	85	
s_{wi},%	20	
c_o, 1/psi	$2x10^{-6}$	
c_w, 1/psi	$3x10^{-6}$	
c_f, 1/psi	$2x10^{-5}$	
c_t, 1/psi	$2.285x10^{-5}$	
B_o, bbl/STB	1.20	1.10
B_w, bbl/STB	1.00	1.05
r_F, ft	1000	300

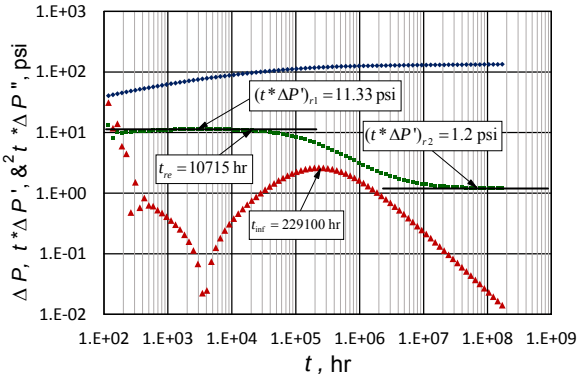

Figure-9. Log-log plot of pressure, pressure derivative and second pressure derivative versus time for example 1.

$$r_F = \frac{1}{2820.627}\sqrt{\frac{(3115.62)(10715)}{(0.2)(1)(2.285\times10^{-5})}} = 958.22 \text{ ft}$$

The time value from the maximum point found on the second pressure derivative -t_{inf}=229100 hr-is also replaced to estimate the invaded front position Equation (20);

$$r_F = \frac{1}{13253.96}\sqrt{\frac{(3115.62)(229100)}{(0.2)(1)(2.285\times10^{-5})}} = 942.93 \text{ ft}$$

3.1.2 Solution by conventional analysis

The following information was read from Figure-10:

$t_x = 230000$ hr

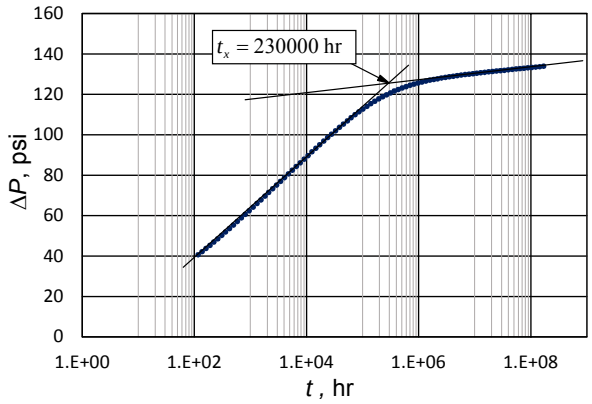

Figure-10. Pressure against the logarithm of the time plot for example 1.

By replacing the time value read on Equation (22), it provides:

$$r_F = \frac{1}{13507.6}\sqrt{\frac{(3115.62)(230000)}{(0.2)(1)(2.285\times10^{-5})}} = 927.04 \text{ ft}$$

3.2 SIMULATED EXAMPLE 2

Figures 11 and 12 contain the data required for example 2. Also, find the effective water permeability, effective oil permeability, and the invaded front position.

3.2.1 Solution by *TDS* technique

The following information was read from Figure-11:

$(t^*\Delta P')_{r1} = 2.5$ psi $(t^*\Delta P')_{r2} = 9.85$ psi
$t_{re} = 104.71$ hr $t_{inf} = 5011.87$ hr

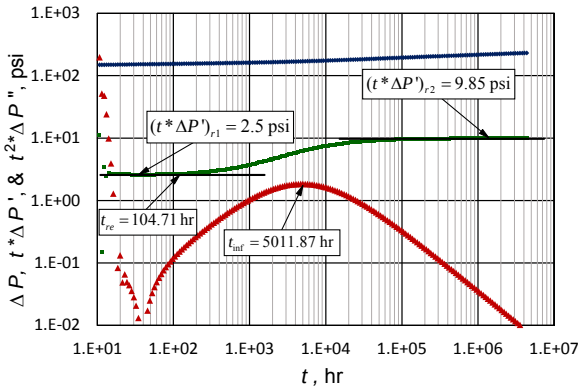

Figure-11. Pressure, pressure derivative and second pressure derivative versus time log-log plot for example 2.

The point read on the pressure derivative during the radial flowalong the water zoneis used to determine effective water permeability from Equation (12);

$$k_w = \frac{70.6(0.25)(6000)(2)(1.05)}{(30)(2.5)} = 2965.2 \text{ md}$$

And the point read on pressure derivative during the radial flow in oil regionis used to determine effective oil permeability from Equation (16);

$$k_o = \frac{70.6(6000)(0.15)(1.05)}{(30)(9.85)(0.25)} = 903.11 \text{ md}$$

Then, using the time at which the radial flow in the water zone ends, the invaded front position is found from Equation (18);

$$r_F = \frac{1}{532.775}\sqrt{\frac{(2965.2)(104.71)}{(0.1)(2)(2.285\times10^{-5})}} = 379.83 \text{ ft}$$

The time value from the maximum point found on the second pressure derivative is replaced to estimate again the invaded front position Equation (20);

$$r_F = \frac{1}{4679.05}\sqrt{\frac{(2965.2)(5011.87)}{(0.1)(2)(2.285\times10^{-5})}} = 385.40 \text{ ft}$$

3.2.2 Solution by conventional analysis

The following information was read from Figure-12:

$t_x = 4000$ hr

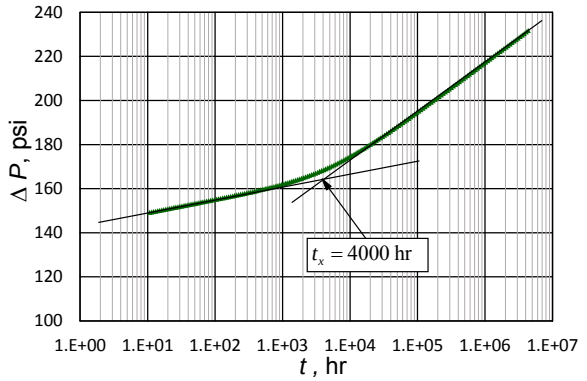

Figure-12. Pressure against the logarithm of thetime plot for example 2.

By replacing the time value read on Equation (22), will provide:

$$r_F = \frac{1}{5333.05}\sqrt{\frac{(2965.2)(4000)}{(0.1)(2)(2.285\times10^{-5})}} = 302.08 \text{ ft}$$

4. COMMENTS ON THE RESULTS

The results obtained for the determination of the invaded front position using both ways: *TDS* technique and conventional analysis were satisfactory, since the developed expression sallow obtaining absolute deviation errors less than 10%.

Regarding mobility ratio greater than unit, addressed in simulated example 1, the best results were obtained by Equation (18) and (20), which use *TDS* technique and imply an absolute deviation error less than 6%.Otherwise, considering a mobility ratio less than one, simulated in example 2, the best results were obtained by Equation (22), which use conventional analysis and supply an absolute deviation error less than 1%.

However, all the expressions give results with deviation errors less than 10% to estimate the radius on the invasion front.

Because of the line-source solution of the pressure model, the development of early radial flow is not very accurate for favorable mobility ratio cases, then, equations are not so accurate for such case.

5. CONCLUSIONS

New expressions are introduced for determination of the invaded front position from transient pressure analysis using both *TDS* technique and straight-line conventional analysis (semilog plot). The equations were successfully tested providing errors lower than 1% in the best case and lower than 10% in the worst scenario.

NOMENCLATURE

B	Oil volume factor, rb/STB
C	Wellbore storage coefficient, bbl/psi
c_f	Reservoir compressibility, psi^{-1}
c_o	Oil compressibility, psi^{-1}
c_t	Totalsystemcompressibility,psi^{-1}
c_w	Watercompressibility,psi^{-1}
c_1	Total system compressibility of the invaded zone, psi^{-1}
c_2	Total system compressibility of the uninvaded zone, psi^{-1}
h	Reservoir thickness, ft
k	Formation permeability, md
P	Pressure, psi
q	Oil flow rate, BPD
r_F	Radius on the invasion front, ft
r_{FD}	Dimensionless waterfront radius, r_F/r_w
r_w	Wellbore radius, ft
S	Saturation
t	Injection time, hr
Δt	Falloff time, hr
ΔP	Pressure drop, psi
t_D	Dimensionless time
t_D*P_D'	Dimensionless pressure derivative
$t_D^2*P_D$''	Dimensionless second pressure derivative
$t*\Delta P$'	Pressure derivative, psi
$t^2*\Delta P$''	Second pressure derivative, psi

Greeks

Δ	Change, drop
ϕ	Porosity, fraction
μ	Viscosity, cp

Suffices

D	Dimensionless
F	Front
inf	Inflexion
o	Oil
r	Radial
re	Radial ends
ro	Relative to oil
rw	Relative to water
$r1$	Radial flow in region 1, water zone
$r2$	Radial flow in region 2, oil flow
wb	Moving front
w	Water, well, wellbore
wi	Initial water
x	Intersection of the two radial semilog lines

REFERENCES

Habte A. D. and Onur M. 2014, June 1. Laplace-Transform Finite-Difference and Quasistationary Solution Method for Water-Injection/Falloff Tests. Society of Petroleum Engineers. doi: 10.2118/168221-PA.

Banerjee R., Thompson L. G. and Reynolds A. C. 1998, December 1. Injection/Falloff Testing in Heterogeneous Reservoirs. Society of Petroleum Engineers. doi: 10.2118/52670-PA.

Bratvold R. B. and Horne R. N. 1990, September 1. Analysis of Pressure-Falloff Tests Following Cold-Water

Injection. Society of Petroleum Engineers. doi: 10.2118/18111-PA.

Escobar F. H., Martinez J. A. and Bonilla L. F. 2011. Pressure and Pressure Derivative Analysis Different of Type-Curve Matching For Thermal Recovery Processes. CT&F. 4(4): 23-35.

Hachlaf H., Tiab D. and Escobar F. H. 2002, January 1. Effect of Variable Injection Rate on Falloff and Injectivity Tests. Society of Petroleum Engineers. doi: 10.2118/76714-MS.

Jokhio S. A., Tiab D., Abdessalam H. and Escobar F. H. 2001, January 1. Pressure Fall-Off Analysis in Water Injection Wells Using the Tiab's Direct Synthesis Technique. Society of Petroleum Engineers. doi: 10.2118/70035-MS.

Woodward D. K. and Thambynayagam R. K. M. 1983, January 1. Pressure Build-Up and Fall-Off Analysis of Water Injection Tests. Society of Petroleum Engineers.

Levitan M. M. 2002, January 1. Application of Water Injection/Falloff Tests for Reservoir Appraisal: New Analytical Solution Method for Two-Phase Variable Rate Problems. Society of Petroleum Engineers. doi: 10.2118/77532-MS.

L. F. Bittencourt Neto J., Vieira Bela R., Pesco S. and Barreto A. 2020, July 20. Pressure Behavior during Injectivity Tests - A Composite Reservoir Approach. Society of Petroleum Engineers. doi:10.2118/198983-MS.

Peres A. M. M., Boughrara A. A., Chen S., Machado A. A. V. and Reynolds A. C. 2004, January 1. Approximate Analytical Solutions for the Pressure Response at a Water Injection Well. Society of Petroleum Engineers. doi: 10.2118/90079-MS.

Peres A. M., Boughrara A. A., and Reynolds A. C. 2006, September 1. Rate Superposition for Generating Pressure Falloff Solutions. Society of Petroleum Engineers. doi:10.2118/90907-PA.

Thambynayagam R. K. M. 1984, January 1. Analytical Solutions for Pressure Buildup andFalloff Analysis of Water Injection Tests of Partially Penetrating Wells: Nonunit Mobility Ratios. Society of Petroleum Engineers. doi:10.2118/12965-MS.

Tiab D. 1995. Analysis of pressure and pressure derivative without type-curve matching: 1 skin and wellbore storage. Journal of Petroleum Science and Engineering. 12. pp. 171-181.